Quadratic correlation filter design methodology for target detection and surveillance applications

Abhijit Mahalanobis, Robert R. Muise, and S. Robert Stanfill

A novel method is presented for optimization of quadratic correlation filters (QCFs) for shift-invariant target detection in imagery. The QCFs are quadratic classifiers that operate directly on the image data without feature extraction or segmentation. In this sense, the QCFs retain the main advantages of conventional linear correlation filters while offering significant improvements in other respects. For example, multiple correlators work in parallel to optimize jointly the QCF performance metric and produce a single combined output, which leads to considerable simplification of the postprocessing scheme. In addition, QCFs also yield better performance than their linear counterparts for comparable throughput requirements. The primary application considered is target detection in infrared imagery for surveillance applications. In the current approach, the class-separation metric is formulated as a Rayleigh quotient that is maximized by the QCF solution. It is shown that the proposed method results in considerable improvement in performance compared with a previously reported QCF design approach and many other detection techniques. The results of independent tests and evaluations at the U.S. Army's Night Vision Laboratory are also presented.

OCIS codes: 100.5010, 100.6740, 100.2000.

1. Introduction

The detection of targets in imagery has been extensively investigated and many techniques have emerged. Some approaches to target detection are based on feature extraction followed by diverse classification techniques such as neural networks[1] and various statistical tools, such as decision trees[2] and support vector machines.[3] Other methods employ segmentation and edge extraction for model-based analysis.[4,5] Each approach has merits and drawbacks depending on the application. The method of interest in this paper is based on correlation filtering. It is well known that the main advantage of linear correlation filters[6–8] is that shift invariance is inherently obtained, and no explicit segmentation and feature extraction is required. Computationally, correlation filters are attractive since they can be efficiently implemented either optically or digitally. The disadvantage is that a large number of linear filters are required to handle a wide range of variations. Moreover, the filters are usually designed separately, and their output is independently processed to select a winner. Searching multiple output planes is often a time-consuming process and prone to decision errors.

To overcome the limitations of linear correlation filters, we address the target detection objective by formulating it as a quadratic correlation filter (QCF) design problem. A major benefit of QCFs is the overall reduction in processing complexity and simplification of the decision process. In Section 2 we show that, although the QCF requires several linear filters in parallel, these branches work together to implement one quadratic filter, and their output is combined into a single detection surface. This greatly simplifies postprocessing complexity as the need to search many separate correlation surfaces is eliminated. Another advantage of QCFs is that they are able to better exploit the second-order statistics of the data. It is well known that quadratic classifiers are optimum for Gaussian distribution. However, even when the data are not necessarily Gaussian we expect QCFs to perform better than their linear counterparts under general conditions.

The issue of finding targets in background clutter is a two-class pattern recognition problem. Consider an input signal $\mathbf{x} = [x(0)\ x(1) \cdots x(N-1)]^T$ that can be either a target (class ω_1) or background (class ω_2).

A. Mahalanobis (abhijit.mahalanobis@lmco.com), R. R. Muise, and S. R. Stanfill are with Lockheed Martin, Mail Stop 450, 5600 Sandlake Road, Orlando, Florida 32819-8907.

Received 16 February 2004; revised manuscript received 10 May 2004; accepted 20 May 2004.

0003-6935/04/275198-08$15.00/0

For now we assume that $\mathbf{x}$ is a purely real signal. The output of the QCF is defined as

$$y = \mathbf{x}^T\mathbf{T}\mathbf{x} = \sum_{i=1}^{N}\sum_{j=1}^{N} t_{ij}x(i)x(j). \quad (1)$$

The coefficient matrix $\mathbf{T} = \{t_{ij}\}$ is square and real but otherwise unrestricted. It should be noted that since $\mathbf{T}$ is not required to be positive definite, output y can be either positive or negative. The idea is to determine $\mathbf{T}$ such that y is positive and as large as possible when $\mathbf{x} \in \omega_1$, and negative or as small as possible when $\mathbf{x} \in \omega_2$.

The use of QCFs in optical correlators for pattern recognition was originally proposed by Gheen[9] and further elaborated by Weber and Casasent[10] as a feature extractor for neural network classifiers. Mahalanobis *et al*. recently reported the design of QCFs for target detection based on the two-class Fukunaga–Koontz transform (FKT).[11] Although this has been proved to be a low-rank approximation to the optimum detector,[12] when the class mixtures are Gaussian, the FKT approach does not explicitly maximize a class-separation metric. As a result under general (non-Gaussian) conditions, the new method proposed in this paper exhibits better QCF performance. Sims and Mahalanobis also investigated the application of QCFs for detection of targets in missile seeker imagery[13] and reported it to be generally better compared with linear correlation filters.

The surveillance application considered in this paper involves searching a large area for all types of target and objects of potential interest. The primary objective is to aid a human operator by rank ordering the detections such that the strongest detections represent true targets whereas smaller (weaker) scores represent clutter objects. The performance of the Rayleigh quotient QCF has been extensively tested on IR surveillance imagery and independently evaluated at the U.S. Army's Night Vision Laboratory. In Section 2 we first present the new QCF design technique that maximizes a class-separation metric formulated as a Rayleigh quotient. This is followed in Section 3 by a review of an efficient architecture that is used to implement the QCF for processing large images. A detailed description of performance results is presented in Section 4 along with a summary of the results of independent tests and evaluations conducted by the Night Vision and Electronic Sensors Directorate (NVESD). Our conclusions and summary are presented in Section 5.

2. Design of Quadratic Correlation Filters by Rayleigh Quotient Optimization

The QCF solution based on the FKT[11] is referred to as the tuned basis filters (TBFs) since the underlying basis set changes with data and is tuned to the specific characteristics of the two classes. Although this approach generally produces good class separation, it does not explicitly optimize a metric for discrimination. Here we introduce a new technique for designing QCFs that enhances discrimination by formulating and maximizing a class-separation metric. Toward this end we assume that the form of the coefficient matrix for the quadratic filter in Eq. (1) is

$$\mathbf{T} = \sum_{i=1}^{N} \mathbf{q}_i\mathbf{q}_i^T, \quad (2)$$

where $\mathbf{q}_i$, $1 \le i \le N$, is a set of linearly independent and unit norm basis vectors. Our objective is to determine these basis functions (and hence $\mathbf{T}$) such that separation between the two classes is maximized. The output of the QCF in response to an input vector $\mathbf{x}$ is given by

$$\phi = \mathbf{x}^T\mathbf{T}\mathbf{x}. \quad (3)$$

The idea is to maximize the separation between the expected values of ϕ for the two classes while reducing an upper bound on the variance of ϕ. The separation between the expected value for the two classes is given by

$$E_1\{\phi\} - E_2\{\phi\} = \sum_{i=1}^{N} \mathbf{q}_i(\mathbf{R}_1 - \mathbf{R}_2)\mathbf{q}_i^T, \quad (4)$$

where $E_i\{\cdot\}$ indicates the expectation operator over the ith class, and $\mathbf{R}_i = E_i\{\mathbf{x}\mathbf{x}^T\}$ is the correlation matrix for class ω_i. The maximization of this term alone, however, results in a solution that does not adequately control the spread of the class statistic. To avoid this, we also seek to minimize

$$E_1\{\phi\} + E_2\{\phi\} = \sum_{i=1}^{N} \mathbf{q}_i(\mathbf{R}_1 + \mathbf{R}_2)\mathbf{q}_i^T. \quad (5)$$

It can be shown that including this term places bounds on the second-order statistics of ϕ and helps to reduce the spread (see Appendix A). To achieve our objectives, we seek $\mathbf{q}_i$ to maximize the ratio

$$J(\mathbf{q}) = \frac{E_1\{\phi\} - E_2\{\phi\}}{E_1\{\phi\} + E_2\{\phi\}} = \frac{\sum_{i=1}^{N} \mathbf{q}_i(\mathbf{R}_1 - \mathbf{R}_2)\mathbf{q}_i^T}{\sum_{i=1}^{N} \mathbf{q}_i(\mathbf{R}_1 + \mathbf{R}_2)\mathbf{q}_i^T}. \quad (6)$$

By taking the derivative of the expression with respect to $\mathbf{q}_i$, we observe that

$$(\mathbf{R}_1 + \mathbf{R}_2)^{-1}(\mathbf{R}_1 - \mathbf{R}_2)\mathbf{q}_i = \lambda_i\mathbf{q}_i. \quad (7)$$

Thus $\mathbf{q}_i$ is an eigenvector of the matrix $(\mathbf{R}_1 + \mathbf{R}_2)^{-1}(\mathbf{R}_1 - \mathbf{R}_2)$ with eigenvalue λ_i. The dominant eigenvector of course maximizes the ratio for the choice of any one vector. The question is how should the remaining $N - 1$ vectors be selected such that $J(\mathbf{q})$ in Eq. (6) is maximized? It turns out that, since $\mathbf{q}_i$ are a set of linearly independent basis vectors, the optimum choice is to select the N eigenvectors of $(\mathbf{R}_1 + \mathbf{R}_2)^{-1}(\mathbf{R}_1 - \mathbf{R}_2)$ in order of decreasing eigenvalues (see Appendix B). Once the eigenvectors of the above matrix are computed, the QCF coefficient matrix $\mathbf{T}$ can be obtained by means of Eq. (2).

It can be shown that the eigenvectors and eigen-

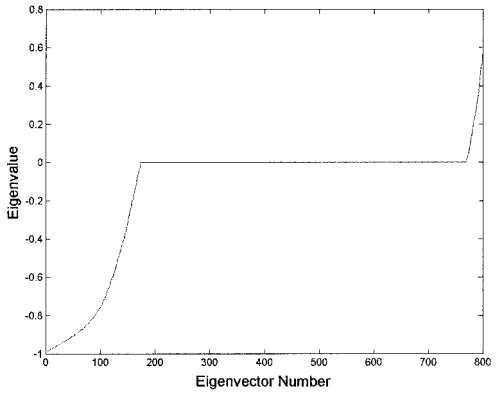

Fig. 1. Typical eigenvalues of $(\mathbf{R}_1 + \mathbf{R}_2)^{-1}(\mathbf{R}_1 - \mathbf{R}_2)$ range between -1 and 1. The eigenvectors that correspond to eigenvalues with large magnitudes are included in the coefficient matrix.

values of $(\mathbf{R}_1 + \mathbf{R}_2)^{-1}(\mathbf{R}_1 - \mathbf{R}_2)$ are related to those of $\mathbf{R}_2{}^{-1}\mathbf{R}_1$. To prove this we observe that

$$\begin{aligned}(\mathbf{R}_1 - \mathbf{R}_2)\mathbf{q}_i = \lambda_i(\mathbf{R}_1 + \mathbf{R}_2)\mathbf{q}_i \\ \Rightarrow \mathbf{R}_1\mathbf{q}_i(1 - \lambda_i) = \mathbf{R}_2\mathbf{q}_i(1 + \lambda_i) \\ \Rightarrow \mathbf{R}_2{}^{-1}\mathbf{R}_1\mathbf{q}_i = \mathbf{q}_i\frac{(1 + \lambda_i)}{(1 - \lambda_i)} = \mathbf{q}_i\gamma_i. \quad (8)\end{aligned}$$

Therefore vectors $\mathbf{q}_i$ are also eigenvectors of $\mathbf{R}_2{}^{-1}\mathbf{R}_1$, but with γ_i as the corresponding eigenvalues. Since both $\mathbf{R}_1$ and $\mathbf{R}_2$ are positive definite, γ_i must be positive. The relationship between eigenvalues implies, however, that $\lambda_i \to -1$ as $\gamma_i \to 0$ and that $\lambda_i \to 1$ if $\gamma_i \to \infty$. It therefore follows that the eigenvalues of $(\mathbf{R}_1 + \mathbf{R}_2)^{-1}(\mathbf{R}_1 - \mathbf{R}_2)$ must range between -1 and 1. An example of the typical distribution of eigenvalues for an 800-dimensional system is shown in Fig. 1. The underlying data used for obtaining this plot are discussed in detail in Section 3.

Let us now consider the ratio

$$\frac{E_1(\phi)}{E_2(\phi)} = \frac{\sum_{i=1}^{N} \mathbf{q}_i{}^T\mathbf{R}_1\mathbf{q}_i}{\sum_{i=1}^{N} \mathbf{q}_i{}^T\mathbf{R}_2\mathbf{q}_i}. \quad (9)$$

It is easy to show that vectors $\mathbf{q}_i$ that maximize this ratio are the eigenvectors of $\mathbf{R}_2{}^{-1}\mathbf{R}_1$ as well. Therefore the solution that maximizes $J(\mathbf{q})$ in Eq. (6) also maximizes the ratio in Eq. (9). As a result $E_1(\phi)$ is as large as possible compared with $E_2(\phi)$, which increases the separation $E_1(\phi) - E_2(\phi)$. Thus by selecting $\mathbf{q}_i$ to be the dominant eigenvectors of $\mathbf{R}_2{}^{-1}\mathbf{R}_1$ [and hence also of $(\mathbf{R}_1 + \mathbf{R}_2)^{-1}(\mathbf{R}_1 - \mathbf{R}_2)$], we ensure that the means of the statistics are well separated. We refer to the QCF solution obtained here as the Rayleigh quotient (RQ) QCF.

A. Methodology for Selecting Eigenvectors to Maximize Class Separation

The separation between the classes in Eq. (4) is a sum of N independent terms. We can therefore maximize the overall separation along each direction one at a time. Based on Eq. (7) we observe that

$$\mathbf{q}_i{}^T(\mathbf{R}_1 - \mathbf{R}_2)\mathbf{q}_i = \lambda_i\mathbf{q}_i{}^T(\mathbf{R}_1 + \mathbf{R}_2)\mathbf{q}_i \quad (10)$$

or

$$\frac{\mathbf{q}_i{}^T(\mathbf{R}_1 - \mathbf{R}_2)\mathbf{q}_i}{\mathbf{q}_i{}^T(\mathbf{R}_1 + \mathbf{R}_2)\mathbf{q}_i} = \lambda_i. \quad (11)$$

Since this is just one of the terms in the definition of $J(\mathbf{q})$ in Eq. (6), we can state that the value of the optimized metric based on any one eigenvector is

$$\frac{E_1\{\phi\} - E_2\{\phi\}}{E_1\{\phi\} + E_2\{\phi\}} = J(\mathbf{q}_i) = \frac{\mathbf{q}_i(\mathbf{R}_1 - \mathbf{R}_2)\mathbf{q}_i{}^T}{\mathbf{q}_i(\mathbf{R}_1 + \mathbf{R}_2)\mathbf{q}_i{}^T} = \lambda_i. \quad (12)$$

We can now derive an expression for the separation between the classes along the ith direction. From Eq. (12) we observe that

$$E_1(\phi)\frac{1 - \lambda_i}{1 + \lambda_i} = E_2(\phi). \quad (13)$$

Substituting for $E_2(\phi)$ in terms of $E_1(\phi)$, the separation between the classes along the ith direction is seen to be

$$E_1(\phi) - E_2(\phi) = E_1(\phi)\left[1 - \frac{1 - \lambda_i}{1 + \lambda_i}\right]. \quad (14)$$

The relative separation between the two classes with respect to $E_1(\phi)$ is

$$\frac{E_1(\phi) - E_2(\phi)}{E_1(\phi)} = \left(1 - \frac{1 - \lambda_i}{1 + \lambda_i}\right) = \frac{2\lambda_i}{1 + \lambda_i}. \quad (15)$$

Since we are interested in making the magnitude of the separation large, the sign on the right-hand side of Eq. (15) is not important. Thus we note that the separation along each direction will be as large as possible if we choose eigenvectors that correspond to eigenvalues close to -1 or $+1$. Specifically, we deduce that $E_1(\phi) = 0$ but $E_2(\phi)$ is as large as possible when $\lambda_i = -1$. Similarly $E_2(\phi) = 0$ but $E_1(\phi)$ is as large as possible when $\lambda_i = 1$. Finally, $E_1(\phi) = E_2(\phi)$ when $\lambda_i = 0$ and the classes are not separable.

Based on the above reasoning, we include the eigenvectors with relatively large (negative or positive) eigenvalues in the definition of the $\mathbf{T}$ matrix, whereas eigenvectors that correspond to eigenvalues close to 0 are omitted. The sign of the separation along each direction is easily reconciled by scaling the eigenvectors that correspond to negative eigenvalues by -1. One way to implement this is to split the coefficient matrix $\mathbf{T}$ into two terms such that

$$\mathbf{T} = \sum_{i=1}^{N_1} \mathbf{q}_i\mathbf{q}_i{}^T - \sum_{i=1}^{N_2} \mathbf{p}_i\mathbf{p}_i{}^T, \quad (16)$$

where $\mathbf{p}_i$ and $\mathbf{q}_i$ eigenvectors correspond to negative and positive eigenvalues, respectively.

In practice, it is preferable to compute the eigenvectors of $(\mathbf{R}_1 + \mathbf{R}_2)^{-1}(\mathbf{R}_1 - \mathbf{R}_2)$ rather than those of

$\mathbf{R}_2^{-1}\mathbf{R}_1$. This is true in particular when the matrices are less than full rank. The reason is that the singular directions of $\mathbf{R}_2^{-1}\mathbf{R}_1$ are difficult to separate from basis functions that best represent class 2 (i.e., eigenvectors that represent class 2 also exhibit small eigenvalues). Using the proposed construction, eigenvectors for class 1 and class 2 are neatly mapped toward eigenvalues of 1 and -1, respectively, and are well separated from the singular values. It is true that the eigenvectors that represent class 2 can be obtained by decomposing $\mathbf{R}_1^{-1}\mathbf{R}_2$. The numerical computations cannot however yield a set that is exactly orthogonal with respect to eigenvectors of $\mathbf{R}_2^{-1}\mathbf{R}_1$.

B. Efficient Implementation of Quadratic Correlation Filters

Consider now the problem of processing an entire two-dimensional (2-D) image using a QCF. Let us assume that vector $\mathbf{z}$ is obtained by lexicographically reordering a relatively small window of row and column size $r \times c$ within a much larger image of size $R \times C$.[1] Typical sizes of real-world images can be 480×720 pixels (or larger), whereas the window size for $\mathbf{x}$ could be 20×40, chosen to be approximately the size of targets of interest. The complexity of the direct computation necessary to evaluate the expression in Eq. (1) at all overlapping $r \times c$ subregions of the image is rather large. We therefore seek an efficient architecture for obtaining the full correlation of the input scene and the quadratic filter.

Denoting the dimensionality of the space by $d = r \cdot c$, let us assume that the $d \times d$ coefficient matrix $\mathbf{T}$ of rank N in Eq. (2) can be expressed as $\mathbf{T} = \mathbf{F}\mathbf{F}^T$, where $\mathbf{F} = [\mathbf{q}_1\ \mathbf{q}_2 \cdots \mathbf{q}_N]$ is a $d \times N$ matrix ($N \le d$). We note that the output of the quadratic filter can be expressed as

$$y = \mathbf{z}^T\mathbf{T}\mathbf{z} = \mathbf{z}^T\mathbf{F}\mathbf{F}^T\mathbf{z} = \mathbf{v}^T\mathbf{v}, \tag{17}$$

where $\mathbf{z}$ is an $r \times c$ subregion of the image and $\mathbf{v} = [v_1\ v_2 \cdots v_N]^T$ is a vector of the projection of $\mathbf{z}$ on the N columns of $\mathbf{F}$. Clearly, $\mathbf{v}$ is a function of the spatial region of the image that is represented by $\mathbf{z}$. The question is how the elements of $\mathbf{v}$ can be computed over the entire scene by use of efficient signal processing methods. Let $x(m, n)$ represent the full image to be processed. Furthermore, let us reorder the elements of $\mathbf{q}_i$ into an $r \times c$ mask $f_i(m, n)$. It is then easy to see that the values of v_i (i.e., ith element of $\mathbf{v}$) for all locations within the image can be obtained by means of the 2-D correlation of $f_i(m, n)$ and $x(m, n)$ as

$$v_i(m, n) = x(m, n) \otimes f_i(m, n), \qquad 1 \le i \le N, \tag{18}$$

where the $\otimes$ indicates the 2-D correlation operation. Here we have expressed v_i along with the indices (m, n) to indicate that it is a function of the location of $\mathbf{z}$ in the image. The samples of $v_i(m, n)$ can be viewed as a partial result at each point in the image obtained by projecting the $r \times c$ region of the image centered at that point on $\mathbf{q}_i$. To obtain the quadratic term in Eq. (17) for all the points in the image, it now remains to square the pixel surfaces of partial results and add them. Therefore, the output of the quadratic filter for all the points in the image is given by

$$y(m, n) = \sum_{i=1}^{N} |v_i(m, n)|^2 = \sum_{i=1}^{N} |x(m, n) \otimes f_i(m, n)|^2. \tag{19}$$

The expression in Eq. (19) is a succinct way to express the output of the quadratic filter in response to the full input image. The computations can be readily dealt with by use of an N 2-D cross-correlation operation, each of which can be efficiently implemented either digitally (using fast Fourier transforms) or optically. In fact, a more general form that takes eigenvectors with negative eigenvalues into account is

$$y(m, n) = \sum_{i=1}^{N_2} |x(m, n) \otimes f_i(m, n)|^2 - \sum_{i=1}^{N_1} |x(m, n) \otimes g_i(m, n)|^2, \tag{20}$$

where $f_i(m, n)$ and $g_i(m, n)$ are eigenvectors that correspond to positive and negative eigenvalues, each reshaped into an $r \times c$ mask.

Figure 2 depicts the architecture required to process a full image efficiently with the quadratic filter. Essentially, the input image is correlated with a bank of linear filters (i.e., the columns of matrix $\mathbf{T}$ reshaped into 20×40 kernels) to obtain partial results that are squared and added to obtain the desired quadratic output for each point in the input image. Although several branches of linear filters are required, the architecture shown comprises a single quadratic filter. For a digital implementation with fast Fourier transforms, the number of multiplications required in the architecture is proportional to $N \log(rc)$, where N is the number of branches and $r \times c$ is the size of the filter masks. The architecture in Fig. 2 is general in that any QCF coefficient matrix $\mathbf{T}$ in Eq. (1) can be implemented in this manner, not just the RQ QCF derived in this paper.

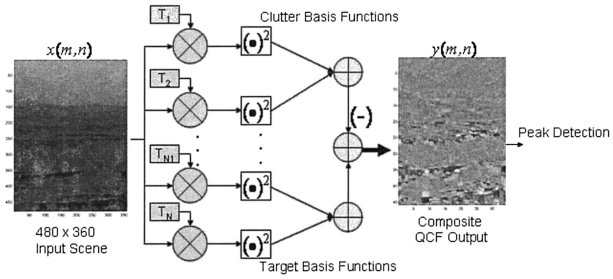

Fig. 2. Efficient QCF architecture is realized by shaping the columns of coefficient matrix $\mathbf{T}$ into 2-D masks, correlating them in parallel with the input image, and adding the squared magnitude output of all the branches.

3. Tests and Performance Evaluations

The goal of the surveillance mission is to process an image rapidly and detect potential targets to cue a

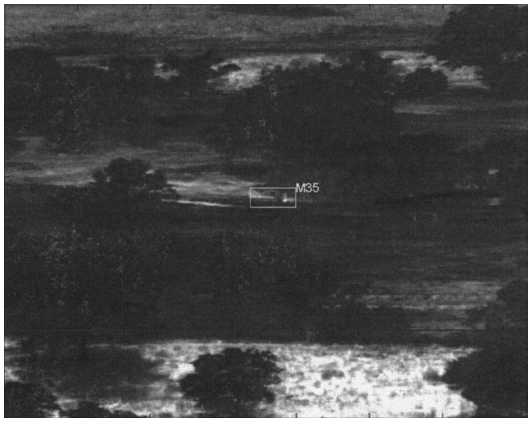

Fig. 3. Typical IR image frame used for evaluating target detection performance.

human operator. The TBF and RQ QCF algorithms have been extensively tested for target detection in such IR imagery provided by the U.S. Army Night Vision Laboratory. We report here results of tests on both sequestered and nonsequestered data. Examples of typical IR imagery obtained with a surveillance sensor are shown in Fig. 3. A large data set (containing over 20,000 images) was provided by the NVESD with ground truth. The data contained over ten types of target observed at diverse ranges, terrains, and times of day. To train the QCFs, we extracted over 5000 images of six different target types from this set and scaled them to fit into a 20×40 window. We used these images to estimate the 800×800 class-1 (target) correlation matrix $\mathbf{R}_1$. Examples of target training images are shown in Fig. 4.

Approximately 15,000 clutter chips were also extracted from the data set. The clutter samples generally contained structure that could be confused with targets. Unlike the class-1 target, however, all the shifted versions of each clutter sample were also included in the estimation of the clutter correlation matrix, because the clutter chips must also be suppressed by the filter. This was done in a computationally efficient manner by use of the autocorrelation function of clutter images. The resulting class-2 (clutter) correlation matrix $\mathbf{R}_2$ has a Toeplitz structure.

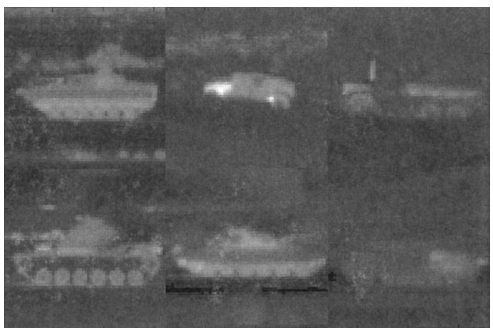

Fig. 4. Typical training images of the six target classes.

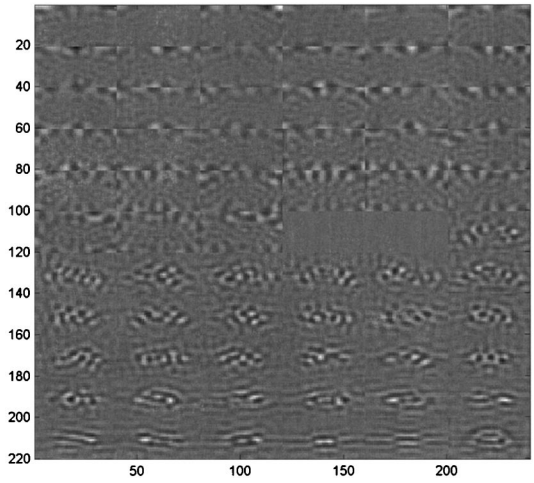

Fig. 5. Each 20×40 kernel in this image is a RQ QCF basis function. The first 33 represent clutter whereas the last 33 represent targets. These are implemented as parallel filters in the architecture in Fig. 2 to obtain the RQ QCF output.

Correlation matrices $\mathbf{R}_1$ and $\mathbf{R}_2$ can be used to obtain eigenvectors $\mathbf{q}_i$ and the corresponding RQ QCF coefficient matrix $\mathbf{T}$ that produces strong peaks at the location of the targets and suppresses clutter as expected. However, to further improve the aim-point (target location) accuracy, a second term must be added to the definition of the class-2 correlation matrix. Essentially, the peaks produced in response to the targets are made narrower by requiring the RQ QCF to suppress the response to all offset positions of the target. Toward this end, a new correlation matrix $\mathbf{R}_S$ is computed based on the shifted positions of the target images. This is added to $\mathbf{R}_2$ to obtain the new class-2 correlation matrix as

$$\hat{\mathbf{R}}_2 = \alpha \cdot \mathbf{R}_2 + \beta \cdot \mathbf{R}_S, \tag{21}$$

where the constants α and β can be used to trade between peak sharpness (or aim-point accuracy) and clutter suppression. It should be noted that unlike $\mathbf{R}_S$, $\mathbf{R}_1$ includes only exactly centered target images (registered on ground truth). Thus the RQ QCF is based on the eigenvectors of $(\mathbf{R}_1 + \hat{\mathbf{R}}_2)^{-1}(\mathbf{R}_1 - \hat{\mathbf{R}}_2)$, and exhibits sharper peaks and improved aim-point accuracy in addition to the ability to suppress clutter.

Examples of some of the RQ QCF basis functions are shown in Fig. 5. The first 33 are eigenvectors (reshaped into 20×40 masks) that correspond to negative eigenvalues and best represent clutter, whereas the last 33 correspond to positive eigenvalues and hence best represent targets. These are essentially the same as the $\mathbf{p}_i$ and $\mathbf{q}_i$ vectors that comprise coefficient matrix $\mathbf{T}$ in Eq. (16). An example of an input scene that contains a target is shown in Fig. 6(a). We processed this scene with the RQ QCF using the basis function shown in Fig. 5 to obtain the output shown in Fig. 6(b). A strong (bright) response is observed at the location that corresponds to the target. The dark regions are produced where structured clutter is strongly suppressed.

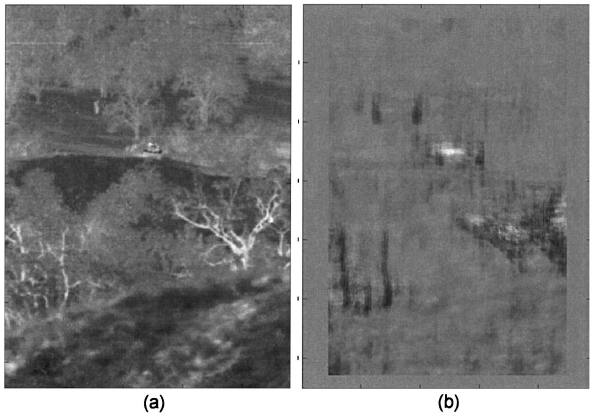

Fig. 6. (a) Input scene is processed by the (b) RQ QCF to produce the output. A strong (bright) response is observed at the location of the target. Dark regions represent where structured clutter has been strongly suppressed.

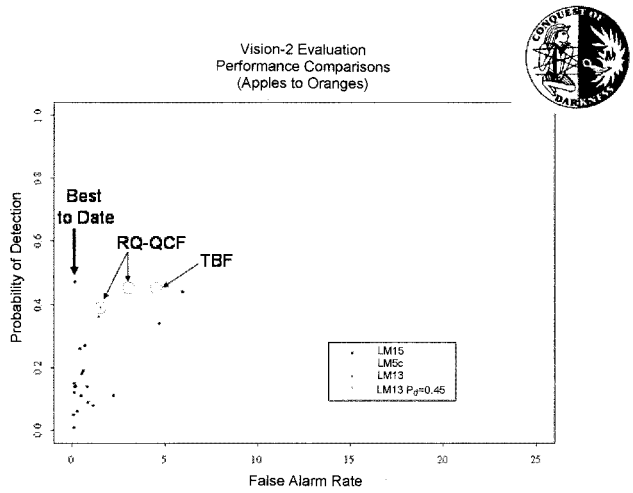

Fig. 8. Results of independent tests taken by the NVESD on the challenging Vision-2 set show that the RQ QCF achieves better performance than most other algorithms tested to date.

To evaluate the performance of the quadratic filter, we selected a subset of 1100 images following criteria adopted by the U.S. Army's NVESD to incorporate a particularly challenging distribution of hard clutter, signal-to-noise ratio, range to target, and times of day. We processed these images using both the TBF reported in Ref. 11 and the RQ QCFs, and the probability of detection (P_d) was compared as a function of the false alarm rate (FAR). The resulting receiver operating characteristic curves are compared in Fig. 7. It is easy to see that the RQ QCF yields considerably better performance (higher P_d at a lower FAR) than the TBF approach. We attribute this improvement in performance to the ability of the RQ QCF to enhance separation between the two classes by maximizing the discrimination metric in Eq. (6).

The RQ TBF method and its variants were also independently evaluated by the NVESD on a challenging sequestered set referred to as the Vision-2 test. The Vision-2 data set is not publicly available, but qualified organizations can be granted access to it by the NVESD. The results of this test are shown in Fig. 8, where the performance of the proposed RQ QCF detection algorithm is compared not only with the TBF QCF, but with algorithms from many other sources. The asterisks in the figure denote the operating points (P_d and the corresponding FAR) achieved by algorithms provided by different research groups or organizations. The NVESD does not disclose the identity of the sources of the algorithms. In general, however, sources from academia, industry, and government laboratories are included.

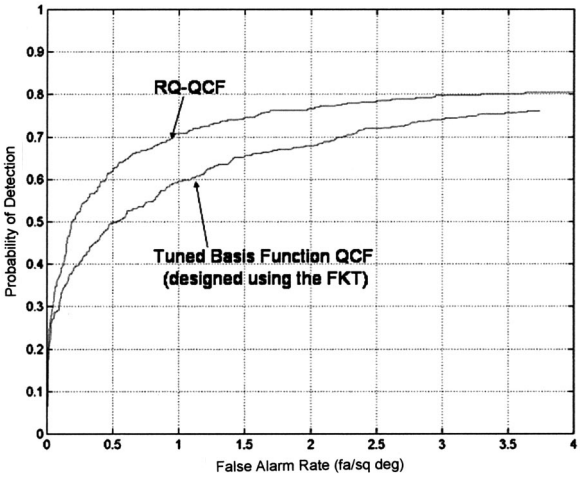

Fig. 7. Comparison of the receiver operating characteristic curves shows that the RQ QCF method performs better for target detection than the TBF QCFs designed by use of the FKT.

The best performance achieved to date with the Vision-2 test is denoted by an arrow in Fig. 8. We note that the highest P_d achieved by any algorithm is approximately in the range of 0.45–0.48. The TBF method (which is also a QCF algorithm) achieved the performance indicated by the LM5c asterisk. Even though the P_d was essentially the same as that of the best, the FAR was higher than desirable [approximately 4.5 false alarm/square degree (fa/sq deg)]. The improved performance achieved by the RQ QCF is indicated by the LM13 and the LM13 $P_d = 0.45$ asterisks. The LM13 asterisk shows that by keeping the P_d at 0.45, the FAR of the QCF approach was reduced to 3 fa/sq deg. The LM13 asterisk is another point on the same receiver operating characteristic that shows a 13% drop in the P_d to 0.39, which allows the QCF FAR to be reduced by greater than 68% (to 1.56 fa/sq deg).

It should be noted that the best-known performance was achieved by an algorithm that embodies knowledge about the test data that is not available to the rest of the algorithms evaluated on this set. Although it is a useful data point for ascertaining a theoretical limit, the evaluators of the NVESD test have labeled it as an apples-to-oranges comparison. In an apples-to-apples comparison, the RQ QCF appears to be the best among all the others tested to

date with the Vision-2 set. The LM13 asterisk shows that, with respect to the group of points that achieve a relatively lower FAR (lower left region of Fig. 8), the RQ QCF algorithm achieves the highest P_d. Similarly, within the loose collection of points that achieve a $P_d \approx 0.45$ (but over a larger span of FARs), the RQ QCF performance indicated by the LM13 asterisk ($P_d = 0.45$) achieves the lowest FAR. Thus, based on the results of the NVESD test, we conclude that not only is the RQ QCF a substantial improvement over the TBFs, but that its performance is better than any others measured to date on the Vision-2 NVESD set and compared with an apples-to-apples basis.

4. Summary

Quadratic correlation filters retain the main advantages of linear correlation filters although they offer significant improvements in other respects. For example, QCFs are also shift invariant, but multiple filters work in parallel to produce a single combined output that considerably reduces postprocessing complexity. A new design method was introduced that optimizes QCF performance by maximizing a class separation metric formulated as a Rayleigh quotient. We have also discussed the rationale for selection of the basis functions and the rank of the detector based on the distribution of the eigenvalues. The main points we have presented in the paper include:

formulation and maximization of a quadratic discrimination (class separation) metric for the detection of targets in clutter;

a methodology for selecting the basis functions to implement the RQ QCF in an efficient image processing architecture; and

extensive evaluation by use of IR surveillance imagery, including the results of independent tests conducted by the NVESD on sequestered imagery.

Future research will be directed toward further generalization of QCFs such as adaptive techniques that can update the clutter statistics on the fly. We also intend to investigate the application and performance of QCFs for multiclass target recognition.

Appendix A

Here we provide a rationale for the claim that the quantity in Eq. (5) reduces the spread (related to the fourth-order moments) of the quadratic performance statistic ϕ. We note that for all real numbers

$$\left(\sum_{i=1}^{N} x_i^2\right)^2 > \sum_{i=1}^{N} x_i^4$$

is true. For real and positive numbers, minimizing x_i reduces $(x_i)^2$ since, if $x_i < x_j$, then $(x_i)^2 < (x_j)^2$. Based on these observations, we note that minimizing $\Sigma\, x_i^2$ will reduce $(\Sigma\, x_i^2)^2$, which is an upper bound on $\Sigma\, x_i^4$. Therefore, minimizing the second-order moment in Eq. (5) reduces an upper bound on the fourth-order moment (and also causes them to become smaller), which in turn reduces the spread (or variance) of statistic ϕ.

Appendix B

Here we substantiate the assertion that the performance objective in Eq. (6) is maximized by selection of $\mathbf{q}_i$ as the N dominant eigenvector of $(\mathbf{R}_1 + \mathbf{R}_2)^{-1}(\mathbf{R}_1 - \mathbf{R}_2)$. Let $\mathbf{A}$ and $\mathbf{B}$ be two symmetric matrices, and let $\mathbf{Q}$ be a matrix whose rows are eigenvectors $\mathbf{q}_i$ of the matrix $\mathbf{A}^{-1}\mathbf{B}$, i.e.,

$$\mathbf{A}^{-1}\mathbf{B}\mathbf{q}_i = \lambda_i \mathbf{q}_i, \qquad \mathbf{Q} = [\mathbf{q}_1\ \mathbf{q}_2\ \Lambda\ \mathbf{q}_N]^T. \tag{B1}$$

It can be shown that

$$\mathbf{Q}\mathbf{A}\mathbf{Q}^T = \mathbf{I}, \qquad \mathbf{Q}\mathbf{B}\mathbf{Q}^T = \Delta, \tag{B2}$$

where Δ is a diagonal matrix with λ_i and the eigenvalues of $\mathbf{A}^{-1}\mathbf{B}$ are its diagonal elements. Thus matrix $\mathbf{Q}$ simultaneously whitens $\mathbf{A}$ and diagonalizes $\mathbf{B}$. This well-known result is often referred to in the literature as simultaneous diagonalization.

Now consider the performance objective $J(\mathbf{q})$ in Eq. (6). We know that $\mathbf{q}_i$ are the eigenvectors of $(\mathbf{R}_1 + \mathbf{R}_2)^{-1}(\mathbf{R}_1 - \mathbf{R}_2)$. The question is how vectors $\mathbf{q}_i$ should be selected so that the function $J(\mathbf{q})$ is maximized? We observe that

$$\begin{aligned}
\sum_{i=1}^{N} \mathbf{q}_i{}^T(\mathbf{R}_1 + \mathbf{R}_2)\mathbf{q}_i &= \text{trace}\{\mathbf{Q}(\mathbf{R}_1 + \mathbf{R}_2)\mathbf{Q}^T\}, \\
\sum_{i=1}^{N} \mathbf{q}_i{}^T(\mathbf{R}_1 - \mathbf{R}_2)\mathbf{q}_i &= \text{trace}\{\mathbf{Q}(\mathbf{R}_1 - \mathbf{R}_2)\mathbf{Q}^T\}.
\end{aligned} \tag{B3}$$

Using the simultaneous diagonalization result, we observed that, if $\mathbf{A} = \mathbf{R}_1 + \mathbf{R}_2$ and $\mathbf{B} = \mathbf{R}_1 - \mathbf{R}_2$, then

$$\mathbf{Q}(\mathbf{R}_1 + \mathbf{R}_2)\mathbf{Q}^T = \mathbf{I}, \qquad \mathbf{Q}(\mathbf{R}_1 - \mathbf{R}_2)\mathbf{Q}^T = \Delta. \tag{B4}$$

Therefore it follows that

$$\begin{aligned}
\sum_{i=1}^{N} \mathbf{q}_i{}^T(\mathbf{R} + \mathbf{R})\mathbf{q}_i &= \text{trace}\{\mathbf{Q}(\mathbf{R}_1 + \mathbf{R}_2)\mathbf{Q}^T\} \\
&= \text{trace}\{\mathbf{I}\} = N, \\
\sum_{i=1}^{N} \mathbf{q}_i{}^T(\mathbf{R} - \mathbf{R})\mathbf{q}_i &= \text{trace}\{\mathbf{Q}(\mathbf{R}_1 - \mathbf{R}_2)\mathbf{Q}\}^T \\
&= \text{trace}\{\Delta\} = \sum_{i=1}^{N} \lambda_i,
\end{aligned} \tag{B5}$$

and the function of interest reduces to

$$J(\mathbf{q}) = \frac{1}{N}\sum_{i=1}^{N} \lambda_i.$$

Thus, the performance metric is equal to the average value of the selected eigenvalues and is maximized by choosing the eigenvectors that correspond to the N largest eigenvalues. It should also be noted that this result holds under any linear transformation of the data since the trace criterion is invariant under linear transformations, a well-known property of the family of similar matrices.

This research was supported by the Defense Advanced Research Projects Agency under the Integrated Sensing and Processing Phase I (Multiscale Automatic Target Recognition Phase II) program. The authors also gratefully acknowledge the technical evaluations and feedback obtained from Richard Harr and Clare Walters at the NVESD.

References

1. L. A. Chan, S. Z. Der, and N. M. Nasrabadi, "Neural based target detectors for multi-band infrared imagery," in *Image Recognition and Classification: Algorithms, Systems, and Applications*, B. Javidi, ed. (Marcel Dekker, New York, 2002), pp. 1–36.
2. J. H. Friedman, "Greedy function approximation: a gradient boosting machine," Ann. Stat. **29,** 1189–1232 (2001).
3. H. Drucker, C. J. C. Burges, L. Kaufman, A. Smola, and V. Vapnik, "Support vector regression machines," Adv. Neural Inf. Process. Syst. **9,** 155–161 (1997).
4. B. Bhanu and J. Ahn, "A system for model-based recognition of articulated objects," in *Proceedings of the Fourteenth International Conference on Pattern Recognition* (Institute of Electrical and Electronics Engineers, Piscataway, N.J., 1998), Vol. 2, pp. 1812–1815.
5. S. Z. Der, Q. Zheng, R. Chellappa, B. Redman, and H. Mahmoud, "View based recognition of military vehicles in ladar imagery using CAD model matching," in *Image Recognition and Classification: Algorithms, Systems, and Applications*, B. Javidi, ed. (Marcel Dekker, New York, 2002), pp. 151–187.
6. B. V. K. Vijaya Kumar, "Tutorial survey of composite filter designs for optical correlators," Appl. Opt. **31,** 4773–4801 (1992).
7. A. Mahalanobis, B. V. K. Vijaya Kumar, S. Song, S. R. F. Sims, and J. F. Epperson, "Unconstrained correlation filters," Appl. Opt. **33,** 3751–3759 (1994).
8. A. Mahalanobis and B. V. K. Vijaya Kumar, "Polynomial filters for higher order correlation and multi-input information fusion," in *Optoelectronic Information Processing*, B. Javidi and P. Refregier, eds., Vol. PM54 of SPIE Press Monographs (SPIE Press, Bellingham, Wash., 1997), pp. 221–231.
9. G. Gheen, "A general class of invariant quadratic filters for optical pattern recognition," Proc. SPIE **2237,** 19–26 (1994).
10. D. Weber and D. P. Casasent, "Quadratic filters for object classification and detection," in *Optical Pattern Recognition VIII*, D. P. Casasent and T.-H. Chao, eds., Proc. SPIE **3073,** 2–13 (1997).
11. A. Mahalanobis, R. R. Muise, S. R. Stanfill, and A. Van Nevel, "Design and application of quadratic correlation filters for target detection," IEEE Trans. Aerosp. Electron., to be published.
12. X. Huo, M. Elad, A. G. Flesia, R. R. Muise, S. R. Stanfill, J. Friedman, B. Popescu, J. Chen, A. Mahalanobis, and D. L. Donoho, "Optimal reduced-rank quadratic classifiers using the Fukunaga–Koontz transform with applications to automated target recognition," in *Automatic Target Recognition XIII*, F. A. Sadjadi, ed., Proc. SPIE **5094,** 59–72 (2003).
13. S. R. F. Sims and A. Mahalanobis, "Performance evaluation of quadratic correlation filters for target detection and discrimination in infrared imagery," Opt. Eng. (to be published).